

Dielectric and ferroelectric behavior of SBN50 synthesized by solid-state route using different precursors

P.K. Patro^a, A.R. Kulkarni^{a,*}, C.S. Harendranath^b

^a Department of Metallurgical Engineering and Materials Science, Indian Institute of Technology, Bombay, Mumbai 400076, India

^b Sophisticated Analytical Instrument Facility (SAIF), Indian Institute of Technology, Bombay, Mumbai 400076, India

Received 1 December 2003; received in revised form 11 December 2003; accepted 22 December 2003

Available online 6 May 2004

Abstract

In the present study, two different sets of precursors have been used in the synthesis of strontium barium niobate (SBN50) by conventional solid-state route: I. $\text{Sr}(\text{NO}_3)_2$, $\text{Ba}(\text{NO}_3)_2$, Nb_2O_5 and II. SrCO_3 , BaCO_3 and Nb_2O_5 . The formation of SBN50 phase was completed at 1150 °C. The green compacts, of the calcined powder, were sintered at temperatures varying from 1250 to 1350 °C. Microstructural characterization was done using scanning electron microscopy (SEM) and transmission electron microscopy (TEM). The aim was to study the dielectric and ferroelectric behavior depending on the precursors used and the sintering conditions and correlate with microstructure. The synthesis, involving the precursor set-I, showed a duplex microstructure with large number of small grains, of size 10–15 μm , sandwiched between very large grains, of size in the range of 50–200 μm . On the other hand the second set of precursor resulted in a microstructure devoid of duplex nature. The microstructure consisted of polyhedral grains having more or less uniform size. SBN from set-II showed a better dielectric property compared to set-I. The discrepancies in this ferroelectric/dielectric behavior, have been explained in terms of density as well as microstructural differences. © 2004 Elsevier Ltd and Techna Group S.r.l. All rights reserved.

Keywords: Strontium barium niobate; Ferroelectrics; Lead free electroceramics; Dielectric; Duplex-microstructure

1. Introduction

Strontium barium niobate ($\text{Sr}_x\text{Ba}_{1-x}\text{Nb}_2\text{O}_6$, $0.25 \leq x \leq 0.75$, abbreviated as SBN) is a promising lead free ferroelectric-based material, owing to its large pyroelectric [1], electro-optic [2], non-linear optical properties, etc. [3]. The physical and electrical properties vary with composition and sintering conditions. Although single crystal of SBN with varying composition has been used immensely, it finds restricted application because of its difficulty in fabrication and associated high cost. For optical applications, it is desirable that SBN should have a density near to theoretical one and uniform microstructure. But SBN ceramic, with nearly theoretical density, is difficult to obtain during pressureless sintering because of abnormal grain growth [4]. Efforts have been made to obtain high density SBN by

hot pressing [5], double stage sintering [4] and using sintering aids [6]. Alternate synthesis methods such as partial coprecipitation [7], solution combustion [8], coprecipitation [9], sol-gel [10], EDTA-complex chemical route [11], etc. have also been employed to improve its physical, dielectric and microstructural properties.

In this paper, conventional solid-state synthesis route with different precursors, has been adopted to investigate the effect of precursors on the microstructural and dielectric properties.

2. Experimental procedures

The precursors used for synthesis of SBN were Nb_2O_5 (99.99%), $\text{Sr}(\text{NO}_3)_2$ (99%), $\text{Ba}(\text{NO}_3)_2$ (99%), SrCO_3 (99.99%) and BaCO_3 (99 %), procured from Aldrich, USA.

Two sets of SBN were prepared, set-I, from Nb_2O_5 , $\text{Sr}(\text{NO}_3)_2$, $\text{Ba}(\text{NO}_3)_2$ (termed as N-based) and set-II, from Nb_2O_5 , SrCO_3 and BaCO_3 (termed as C-based). The

* Corresponding author. Tel.: +91-22-2576-7636; fax: +91-22-2572-3480.

E-mail address: ajit.kulkarni@iitb.ac.in (A.R. Kulkarni).

stoichiometric amount of the pre dried powder was mixed with automatic agate mortar with methanol as mixing agent. This was the further ball milled using zirconia balls for 24 h. Phase analysis of the calcined powder was done using powder XRD (*Phillips X-pert*), transmission electron microscopy (TEM) (*Phillips CM200*) and scanning electron microscopic (SEM) techniques (*Cambridge Stereo-Scan*) were used to study the particle and grain size as well as morphology. The powders were compacted with 2% PVA as binder and sintered in a resistive heating furnace. The sintered compacts were well polished and metallized with sputtered gold and were further metallized with silver paint. The dielectric constant was calculated from measured parallel plate capacitance, from room temperature to 200 °C in frequency range of 1 kHz to 1 MHz using *SI-1260 Impedance Analyzer* with *SI-1296 Dielectric Interface*. The dielectric constant was calculated from the measured parallel plate capacitance. Ferroelectric hysteresis loop was traced using a *Radiant RT66A Ferroelectric Test System*.

3. Results and discussion

X-ray diffraction study revealed that the SBN50 phase was completely formed at the calcination temperature of 1150 °C for both the sets of samples. The TEM study of the calcined powder showed that the particle size was below 250 nm as shown in Fig. 1a and b. For C-based sample, the particles were nearly of same size with varying shapes and with smooth edges. For the N-based sample, few particles were found to be even in the size range of 50 nm or less, and having sharp corners. A fair degree of agglomeration is also observed in both the samples.

The scanning electron micrograph of the sintered pellets is shown in Figs. 2a–c and 3a–c for C-based and N-based samples, respectively. The micrographs corresponding to the sample sintered at 1250 °C, (Figs. 2a and 3a) shows that the C-based samples have much bigger grains than that of the corresponding N-based sample. The grain size in the C-based sample varied from 15 to 30 μm with large number of pores on the surface. In the corresponding micrograph for N-based SBN in Fig. 3a, the grains are much smaller (of the order of 7 μm) than the C-based sample and are of uniform size and polyhedrons in shape. Fig. 2b, the SEM micrograph of C-based sample sintered at 1300 °C, shows grains of about 50 μm size. The grain compaction is high and there is narrow size distribution. The corresponding micrograph for N-based SBN (Fig. 3b) shows a striking dissimilarity. The figure illustrates the observed duplex microstructure comprising of two distinctly different size ranges. Large number of very small grains of size 10–15 μm are sandwiched between very large grains of size range 50–150 μm . The micrograph indicates that, the grains are well sintered and hence less numbers of pores were observed. Fig. 2c shows the feature similar to that of Fig. 2b with no appreciable change in grain size range. Duplex microstructure can also be seen in Fig. 3c with smaller grains are now rectangular in shape. This micrograph also shows the presence of micro cracks due to internal strains resulting from rectangular shaped elongated grains and thin platelet like grains of size range 50–200 μm .

It is interesting to note that the C-based SBN did not show any abnormal grain growth like the N-based SBN (for the sintering conditions under consideration) although, each of them went through the same processing step. However, similar kind of abnormal grain growth has been reported earlier

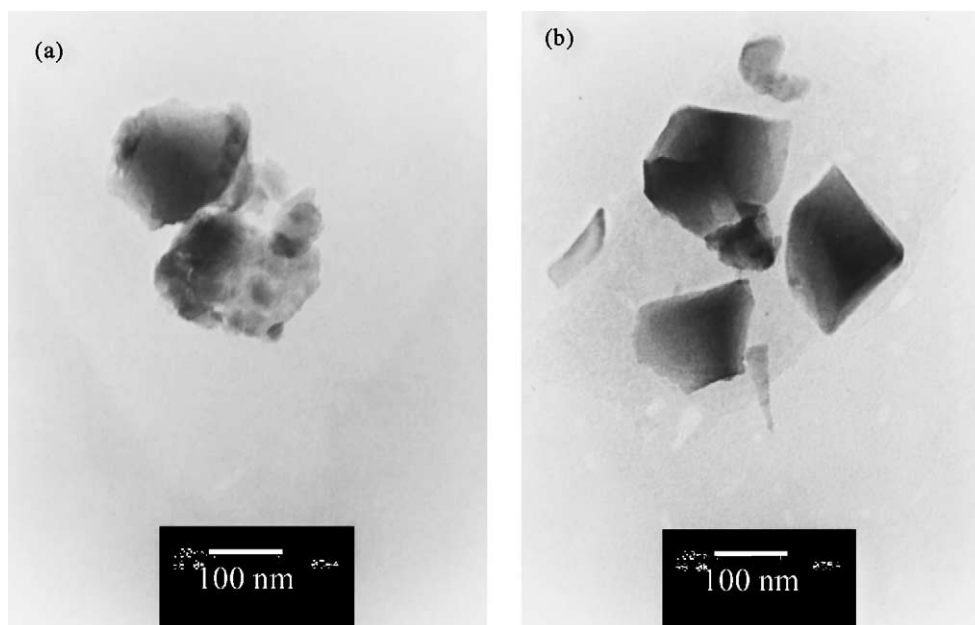


Fig. 1. Transmission electron micrograph of SBN50 powder calcined at 1150 °C (a) C-based (b) N-based.

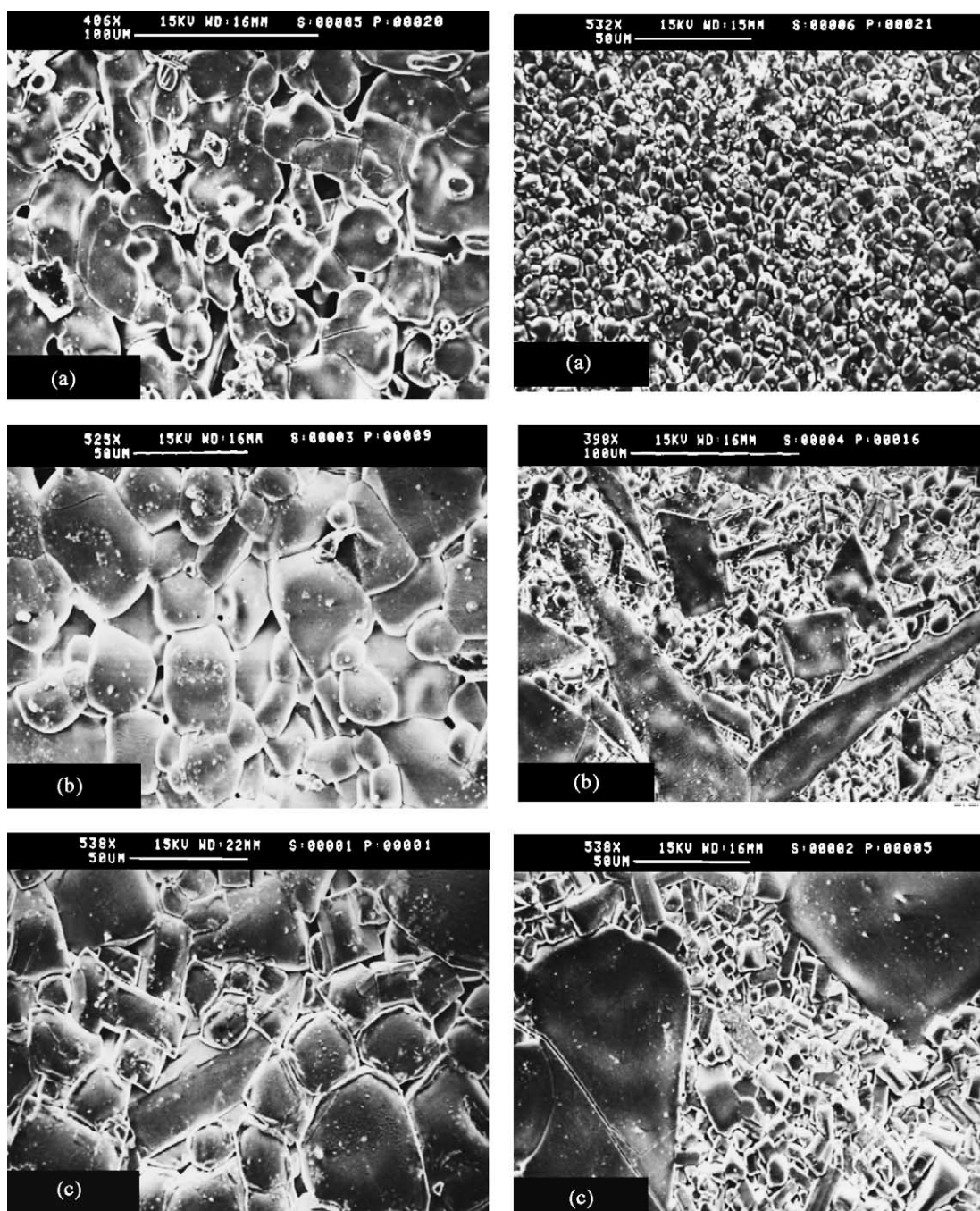


Fig. 2. Scanning electron micrograph of SBN50 for C-based and N-based SBN50 sintered pellets: (a) for 1250 °C; (b) 1300 °C; and (c) 1350 °C.

for C-based SBN with $x = 0.6$ [12]. The exact cause of this abnormality in the grain growth is still not clear. A number of explanations have been put forth for this abnormal grain growth. Takashaki et al. [13] have reported that the abnormal grain growth is due to the liquid phase resulting from local inhomogeneous composition due to partial incomplete of calcination. Fang et al. [14] have suggested that it is due to formation of SrNb_2O_6 , a low melting second phase at the grain boundary. This has been attributed to the decomposition of stoichiometric SBN during ball milling. Lee et al. [12,15] have reported that the formation Nb rich/Ba

poor phase at the grain boundary is the cause of the formation of low melting liquid phase, which in turn results in the formation of the abnormal grain growth. In the present case, however, the C-based SBN does not show abnormal grain growth probably because the additional step of ball milling after calcination has not been employed here. Sr/Ba ratio is also considered to be an important factor in the formation of abnormal grain growth [14]. The lower Sr/Ba ratio employed in the present work has probably contributed to the elimination of abnormal grain growth in C-based SBN. Enhanced grain growth (abnormal) due to ball milling and subsequent

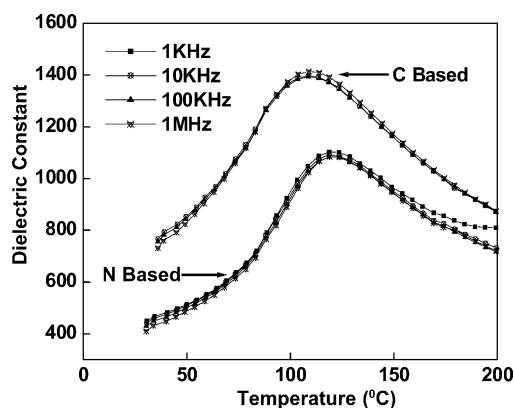


Fig. 3. Dielectric constant vs. temperature plot for C-based and N-based SBN50 at the sintering temperature of 1350 °C.

low melting phase was also observed in our laboratory and will be the subject of discussion in a later communication. It is pertinent to mention here that depending on precursors, there may be some amount of unreacted low melting phase present in the calcined powder resulting in entirely different microstructures. To understand the origin of abnormality in grain growth, X-ray diffraction study of the powders calcined at different temperatures and TEM study on the grain boundary of sintered pellets is underway in authors' laboratory and will be reported elsewhere.

The density of the sintered pellets is listed in the Table 1. For all the cases, the N-based sample has higher density than the C-based samples for the same sintering temperature. In both the cases maximum density was achieved for the 1300 °C sintering temperature. It seems that above 1350 °C uniaxial grain growth has resulted in less compaction. Microcracks have also contributed to lower the density.

The dielectric constant versus temperature plot for the sintering condition of 1350 °C is shown in Fig. 3. This shows a broad dielectric constant versus temperature plot indicating the second order phase transformation (for relaxor ferroelectrics). But the shift of T_c with frequency is not very prominent in both the cases. Porosity correction for the measured dielectric constant was done by using Rushman and

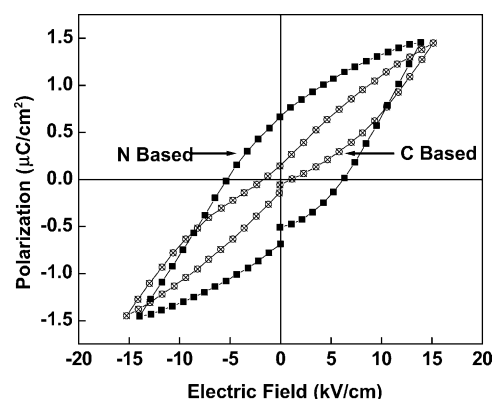


Fig. 4. P - E hysteresis loop trace for C-based and N-based SBN50 at the sintering temperature of 1350 °C.

Strivens equation [16].

$$\varepsilon_{\text{corrected}} = \frac{\varepsilon_{\text{observed}} \times (2 + V_2)}{2(1 - V_2)} \quad (1)$$

The dielectric constant values for other sintering conditions for both the sets of samples are listed in Table 1. This clearly indicates that the C-based SBN shows higher dielectric constant values than the corresponding N-based SBN, for the same sintering conditions. This is in contrast to the observed densities in both the cases. This indicates that, micro cracks due to abnormal grain growth, which is supposed to reduce the density of N-based SBN drastically, has not been so effective but it significantly contributed in the reduction of the dielectric property. PE loop of the pellets sintered at 1350 °C showed low polarizations. However, the N-based samples showed a higher remnant polarization than the C-based for the same electric field as shown in Fig. 4.

4. Conclusions

Strontium barium niobate (SBN50) synthesized from conventional solid-state route, using different precursors, resulted in SBN with different microstructural and dielectric properties. SBN from nitrate precursors (N-based) showed abnormality in grain growth and a duplex microstructure when compared with the SBN from carbonate precursors (C-based). SBN from nitrate precursors is more susceptible for formation of low melting liquid phase.

Acknowledgements

One of the authors (P.K. Patro) is thankful to Council of Scientific and Industrial Research (CSIR), India for financial assistance through Senior Research Fellowship.

References

- [1] A.M. Glass, Investigation of electrical properties of $\text{Sr}_{1-x}\text{Ba}_x\text{Nb}_2\text{O}_6$ with special reference to pyroelectric detection, J. Appl. Phys. 40 (12) (1969) 4699–4713.

Table 1

Variation of density, dielectric constant and T_c (ferroelectric–paraelectric transition temperature) of C-based and N-based SBN50 under different sintering conditions

Sample	Theoretical density (%)	ε_{max} for 1 kHz at T_c		T_c (°C) at 1 kHz
		Observed	Porosity corrected	
1250C ^a	85.4	950	1193	108
1300C	91.1	1143	1311	113
1350C	89.5	1192	1402	108
1250N ^a	91.4	569	650	93
1300N	93.6	644	710	113
1350N	91.3	965	1103	118

^a 1250C: sintered at 1250 °C, C: carbonate precursors. N: nitrate precursors.

- [2] S.T. Liu, R.B. Maciolek, J.D. Zook, B. Rajagopalan, Electro-optic and ferroelectric effect in lanthanum-doped strontium barium niobate single crystals, *Ferroelectrics* 87 (1988) 265–269.
- [3] Y. Xu, H.C. Chen, S.T. Liu, Optical properties and linear electrooptic effect in ferroelectric single crystal KNSBN, *Jpn. J. Appl. Phys.* 24 (2) (1985) 278–280.
- [4] N.S. VanDamme, A.E. Sutherland, L. Jones, K. Bridger, S.R. Winzer, Fabrication of optically transparent and electro-optic strontium barium niobate ceramics, *J. Am. Ceram. Soc.* 74 (8) (1991) 1785–1792.
- [5] K. Nagata, Y. Yamamoto, H. Igarashi, K. Okazaki, Properties of the hot-pressed strontium barium niobate ceramics, *Ferroelectrics* 38 (1–4) (1981) 853–856.
- [6] S.I. Lee, W.K. Choo, Modified ferroelectric high density strontium barium niobate ceramics for pyroelectric applications, *Ferroelectrics* 87 (1988) 209–212.
- [7] P.K. Patro, A.R. Kulkarni, C.S. Harendranath, Microstructure and dielectric properties of strontium barium niobate ceramic, synthesized using partial coprecipitation, *J. Eur. Ceram. Soc.* 23 (8) (2003) 1329–1335.
- [8] P.K. Patro, A.R. Kulkarni, C.S. Harendranath, Combustion synthesis of $\text{Sr}_{0.5}\text{Ba}_{0.5}\text{Nb}_2\text{O}_6$ and effect of fuel on its microstructure and dielectric properties, *Mater. Res. Bull.* 38 (2) (2003) 249–L 259.
- [9] P.K. Patro, R.D. Deshmukh, A.R. Kulkarni, C.S. Harendranath, Synthesis of $\text{Sr}_{0.5}\text{Ba}_{0.5}\text{Nb}_2\text{O}_6$ by coprecipitation method-dielectric and microstructural characteristics, *J. Electroceram.*, in press.
- [10] S. Hirano, T. Yogo, K. Kikuta, K. Ogiso, Preparation of strontium barium niobate by sol–gel method, *J. Am. Ceram. Soc.* 75 (6) (1992) 1697–1700.
- [11] A.B. Panda, A. Pathak, P. Pramanik, Low temperature preparation of nanocrystalline solid solution of strontium–barium–niobate by chemical process, *Mater. Lett.* 52 (3) (2002) 180–186.
- [12] H.Y. Lee, R. Freer, The mechanism of abnormal grain growth in $\text{Sr}_{0.6}\text{Ba}_{0.4}\text{Nb}_2\text{O}_6$ ceramics, *J. Appl. Phys.* 81 (1) (1997) 376–382.
- [13] J. Takahashi, S. Nishiwaki, K. Kodaira, Sintering and microstructure for $\text{Sr}_{0.6}\text{Ba}_{0.4}\text{Nb}_2\text{O}_6$ ceramics, *Ceram. Trans.* 41 (1994) 363–370.
- [14] T.T. Fang, E. Chen, W. Lee, On the discontinuous grain growth of $\text{Sr}_x\text{Ba}_{1-x}\text{Nb}_2\text{O}_6$ ceramics, *J. Eur. Ceram. Soc.* 20 (4) (2000) 527–530.
- [15] M.S. Kim, J.H. Lee, J.J. Kim, H.Y. Lee, S. Cho, Microstructure and dielectric characteristics of tungsten bronze structured SBN70 ceramics: effect of Nb_2O_5 content, *J. Eur. Ceram. Soc.* 22 (13) (2002) 2107–2113.
- [16] D.F. Rushman, M.A. Strivens, The effective permittivity of two-phase system, *Proc. Phys. Soc.* 59 (1947) 1011–1016.